Aerosol and Air Quality Research

ORIGINAL RESEARCH
https://doi.org/10.4209/aaqr.220032

Gasoline Direct Injection Engine Emissions of OC and EC: Laboratory Comparisons with Port Fuel Injection Engine

Jie Zhang[1,2,3], John Liggio[4], Tak W. Chan[2,5], Lin Huang[5], Jeffrey R. Brook[4,6*]

[1] Jiangsu Province Engineering Research Center of Synergistic Control of Pollution and Carbon Emissions in Key Industries, Jiangsu Environmental Engineering Technology Co., Ltd., Nanjing, Jiangsu 210000, China
[2] Emissions Research and Measurement Section, Air Quality Research Division, Environment and Climate Change Canada, Ottawa, Ontario, K1A 0H3, Canada
[3] Jiangsu Collaborative Innovation Center of Atmospheric Environment and Equipment Technology (CICAEET), Nanjing University of Information Science & Technology, Nanjing, Jiangsu 210044, China
[4] Air Quality Research Section, Environment and Climate Change Canada, Toronto, Ontario, M3H 5T4, Canada
[5] Climate Chemistry Measurement and Research, Climate Research Division, Environment and Climate Change Canada, Toronto, Ontario, M3H 5T4, Canada
[6] Dalla Lana School of Public Health and the Department of Chemical Engineering and Applied Chemistry, University of Toronto, Toronto, Ontario M5T 1P8, Canada

ABSTRACT

To better understand carbonaceous aerosol emissions from gasoline vehicles, a gasoline direct injection (GDI) vehicle with and without a gasoline particle filter (GPF) installed and a port fuel injection (PFI) vehicle were tested on a chassis dynamometer using standard emission drive cycles. Carbonaceous particles emitted from the vehicles were collected on quartz filters and analyzed using three different thermal optical protocols to assess the sensitivity of organic carbon (OC) and elemental carbon (EC) emission estimates to the methods, showing OC obtained by the IMPROVE and EC by the NIOSH protocol was the lowest. Compared to the PFI vehicle, the GDI vehicle had higher EC and OC emissions under cold-start cycles by 1415% and 46%, respectively. However, the OC emission from the PFI vehicle was higher than GDI during an aggressive driving cycle by 146%. By considering OC collected on a quartz filter behind a Teflon filter, the emissions from PFI vehicle were found to be more volatile than the GDI vehicle. This is consistent with the OC forming characteristics for GDI and PFI engines, which are pyrolyzed particles from incomplete combustion and incomplete volatilization of fuel droplets, respectively. Generally, the particle phase OC emissions from gasoline engines are more volatile than other sources (e.g., biomass burning), supported by the very low level of pyrolyzed organic carbon (POC) and small differences among protocols in the current study. Once the GDI vehicle was equipped with a GPF, the removal efficiency of EC was > 98%, but OC emissions could increase as a result of regeneration, suggesting that the effect of a GPF on total carbon emitted to the atmosphere needs further evaluation, especially considering the formation of secondary organic aerosol.

Keywords: Gasoline direct injection, Port fuel injection, OC, EC, Gasoline particle filter

OPEN ACCESS

Received: January 20, 2022
Revised: April 5, 2022
Accepted: April 28, 2022

* **Corresponding Author:**
jeff.brook@utoronto.ca

Publisher:
Taiwan Association for Aerosol Research
ISSN: 1680-8584 print
ISSN: 2071-1409 online

1 INTRODUCTION

Gasoline vehicle engines are generally known to emit less black carbon (BC) and total particle mass than those in diesel vehicles (Gordon *et al.*, 2014). However, equipping diesel vehicles with

diesel particle filters (DPF) has significantly reduced particle emissions, which has been shown in the laboratory test (Valverde and Giechaskiel, 2020) and on-road measurements (Preble *et al.*, 2015; Chao *et al.*, 2020). To further improve air quality, it is thus increasing important to focus on reducing emissions from gasoline vehicles. Gasoline direct injection (GDI) vehicles have many advantages over traditional port fuel injection (PFI) vehicles (Munoz *et al.*, 2018) including improved fuel economy, more precise fuel injection control, less fuel pumping loss, higher compression, and charge air cooling (Chan *et al.*, 2014). However, GDI vehicles have also been found to have higher particulate matter (PM) and BC emissions compared to traditional port fuel injection (PFI) vehicles (Saliba *et al.*, 2017; Chan *et al.*, 2014, 2012). The increased PM and BC emissions are due to incomplete gasoline vaporization and combustion, caused by the difference in fuel injection method and mixture preparation (Maricq *et al.*, 2012; Zimmerman *et al.*, 2016b; Chan *et al.*, 2014, 2012). To reduce particle emissions from GDI vehicles, gasoline particle filters (GPF) have been developed and their use is becoming increasingly common (Munoz *et al.*, 2018; Chan *et al.*, 2014, 2012).

The particles emitted by vehicles are primarily composed of carbonaceous chemical species, broadly consisting of organic carbon (OC) and elemental carbon (EC) (Zhang *et al.*, 2009; Lin *et al.*, 2020). The characteristics of carbonaceous aerosols emitted by diesel vehicles have been studied extensively, whereas research on gasoline vehicle particle composition remains limited, with a relatively small number of studies reporting OC and EC emissions (Cai *et al.*, 2017; May *et al.*, 2013; Chan *et al.*, 2016; Lim *et al.*, 2021). OC emissions are complex, given that they are a mixed state of both particle and gas phase organic compounds, with semivolatile organic compounds (SVOC) dynamically partitioning between phases (Miersch *et al.*, 2019). Such partitioning depends upon exhaust and ambient air conditions such as temperature and molecular structure, including the influence of rapid atmospheric oxidation (Zhang *et al.*, 2013, 2016). This significantly complicates the sampling and measurement of OC emissions and assessment of their overall impact on ambient PM levels. The amount of gaseous SVOC and intermediate volatility species (IVOC), which are, at least partially adsorbed on a quartz filter when sampling, can be estimated by measuring OC on a quartz filter behind a Teflon filter (QBT) (May *et al.*, 2013; Zhang *et al.*, 2013, 2016; Chow *et al.*, 2001; Cheng *et al.*, 2010).

In order to help understand filter-based OC measurements, the different laboratory methods, which do affect the OC and EC emissions reported, are important to consider. Measurement consistency, or at least an understanding of the causes of differences between emissions data that may have relied on different laboratory methods, is necessary improve emission inventories, potentially leading to more confidence in model predictions, source apportionment studies and radiative forcing calculations (Huang *et al.*, 2006; Andreae *et al.*, 2005). Multiple thermal-optical protocols for OC and EC analysis exist. The National Institute for Occupational Safety and Health (NIOSH) (Birch and Cary, 1996) protocol has been evaluated by the U.S. EPA for measuring quartz filter samples for the national monitoring network and is also commonly used to measure OC and EC from source samples (Chow *et al.*, 2001). The Interagency Monitoring of Protected Visual Environment (IMPROVE) protocol (Chow *et al.*, 2001) is also widely applied for ambient and emission source carbonaceous aerosols measurement. Other thermal optical protocols include the European Supersites for Atmospheric Aerosol Research (EUSAAR) (Chiappini *et al.*, 2014), Gwangju Institute of Science and Technology (GIST) (Jung *et al.*, 2011) and EnCan Total-900 protocol (ECT9) (Huang *et al.*, 2006).

In studies comparing OC and EC quantification under different measurement protocols, differences of up to a factor of two have been found for the relative OC and EC amounts ('OC/EC split'), which arises from use of different heating temperatures and dwell times at each temperature step (Chiappini *et al.*, 2014; Chow *et al.*, 2005; Cheng *et al.*, 2014; Giannoni *et al.*, 2016). The magnitude of the differences in the OC/EC split among different protocols also depends upon the composition of the particles being tested (Chiappini *et al.*, 2014).

The current study was designed to characterize carbonaceous aerosols emitted from GDI and PFI vehicles and the effects of a GPF on GDI emissions. The effects of engine type and vehicle operating conditions or cycles (e.g., cold or hot start, acceleration and speed) on OC and EC measurements are reported with a focus on the relative importance of gas phase OC (i.e., SVOC) adsorption on the quartz filters. This study also quantified the effects of three different thermal-optical measurement protocols (Chow *et al.*, 2001; Huang *et al.*, 2006; Chow *et al.*, 2005) on the results, allowing other researchers to compare their results with various protocols.

2 METHODS

2.1 Vehicles and Driving Cycle Setting

The experiment was carried out on two light-duty passenger cars: a 2011 2.4 L Hyundai Sonata with a GDI engine and a 2010 2.4 L Volvo S40 with a PFI engine. During the experiment, the GDI vehicle was tested with and without a gasoline particle filter (GPF), which are referred as GDI+GPF and GDI, respectively. Descriptions and specifications of the two vehicles and the GPF are summarized in Chan *et al.* (2012, 2014). The emission experiments were conducted in a chassis dynamometer emissions measurement facility using three test cycles: (1) U.S. Federal Test Procedure (FTP-75), (2) FTP-72, and (3) US06 Supplemental Federal Test Procedure (US06). Information relating to these cycles are described in the Table S1, Figs. S1–S3 and elsewhere (Chan *et al.*, 2014). Briefly, The FTP-75 represents city driving conditions, consisting of a cold-start, urban, and hot-start phases, where the cold- and hot-start phases are identical. The FTP-72 is a hot-start cycle, consisting only of the last two phases of the FTP-75. The US06 drive cycle simulates the aggressive driving condition (Maricq *et al.*, 2013).

2.2 Particle Emissions Sampling

The exhaust from vehicles was diluted continuously using charcoal and high efficiency particulate air (HEPA)-filtered room air and then introduced into a full-flow constant-volume sampling (CVS) dilution tunnel. Two filter packs were utilized in parallel to sample diluted exhaust from the dilution tunnel using an isokinetic sampling technique at 16.7 L min^{-1} onto a 47 mm diameter pre-fired quartz filters over the entire drive cycle for OC and EC analysis. One of the filterpacks contained a single 47 mm bare quartz filter (Q) and the other contained a 47 mm Teflon filter followed by QBT. Q and QBT integrated samples were collected for each vehicle and test cycle. The OC determined from the QBT is assumed here to estimate the volatility of the particle emissions, since it represented the gas phase OC not trapped by Teflon filter (Cheng *et al.*, 2010). While previous studies have used OC on QBT as a positive artifact correction (Cheng *et al.*, 2010), this study found negative OC of Q-QBT, since a negative artifact (i.e., particle phase SVOC evaporated from the front filter) is also captured on QBT (Zhang *et al.*, 2013, 2016). Therefore, in this paper we use OC on QBT independently and also consider subtracting OC on QBT from Q.

Emissions of other gaseous phase pollutants (CO, CO_2, NO_x and THC) were also measured as given in Table S2. Repeat tests for these gaseous pollutants were performed for most of the cycles to assess variability among tests with the average values and standard deviations shown in Table S2. The differences for the gaseous pollutants between tests for CO, CO_2, NO_x and THC were 15%, 2%, 21% and 8%, respectively. We assume that a similar variability was likely to be present in the OC and EC emissions, and thus obtained Q and QBT samples once for each cycle and engine configuration.

2.3 Carbonaceous Aerosol Measurement Methods

The quartz filters (Q and QBT) were analyzed using three thermal optical protocols. The details are provided in organic carbon. Briefly, these included: (1) IMPROVE where the reflectance signal was used to determine the OC/EC split (i.e., thermal optical reflectance, TOR) (Chow *et al.*, 2001); (2) NIOSH 5040 protocol for thermal optical transmission (TOT) (Giannoni *et al.*, 2016); and (3) ECT9 (Huang *et al.*, 2006). In the ECT9 protocol, the quartz filter was heated stepwise to temperatures of 550°C and 870°C in a pure helium environment to determine OC, including low molecular weight non-refractory organic carbon and pyrolyzed organic carbon (POC) detected at each temperature (Huang *et al.*, 2006). Then the environment was shifted to 10% O_2/90% He, and the filter was heated to 900°C to determine EC. By using the high inert mode temperature, the remained POC could be detected as EC are negligible (Huang *et al.*, 2006). Each protocol also follows different temperature-ramping sequences (Table S3). The IMPROVE protocol was conducted with a DRI 2001 thermal-optical carbon analyzer, and the NIOSH 5040 and ECT9 protocols were carried out with a Sunset Laboratory thermal-optical-transmittance analyzer. The OC and EC results for each protocol are compared in the Table S4.

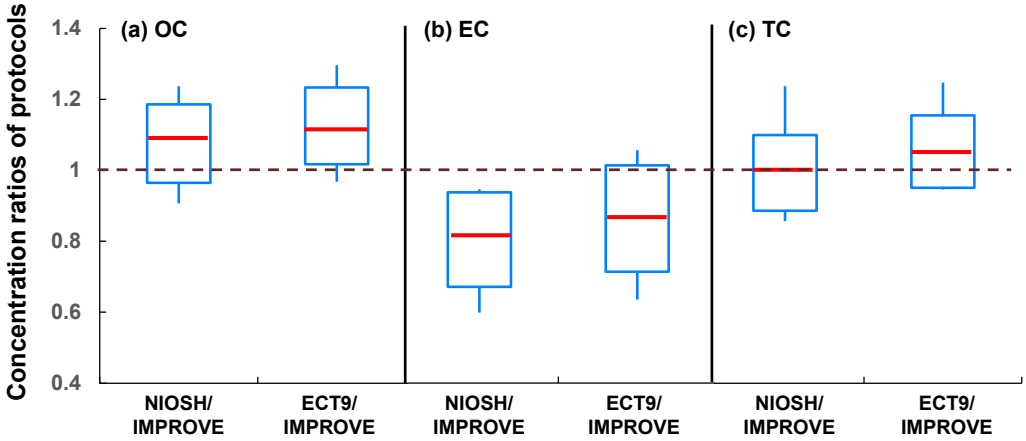

Fig. 1. Comparison of the relative (a) OC, (b) EC and (c) TC concentrations measured by the NIOSH and ECT9 protocol with respect to IMPROVE. The edges of boxes indicate the 25th and 75th percentile, the whiskers extend to the 10th and 90th percentile, and the central (red) lines on the boxplots are averaged data.

3 RESULTS AND DISCUSSION

3.1 Comparison of the OC/EC Protocols

Fig. 1 summarizes the relative OC, EC, and total carbon (TC) for the NIOSH and ECT9 with respect to IMPROVE. In comparison, the IMPROVE and NIOSH protocols generally gives similar TC amount, while the ECT9 protocol results in higher TC than the IMPROVE protocol, but by less than 10%. This overall agreement is in accordance with other studies, which demonstrated that the variance in TC among different protocols was generally less than 10% (Chow *et al.*, 2005; Khan *et al.*, 2012). OC obtained by the IMPROVE protocol was generally the lowest among the three protocols, followed by NIOSH and then ECT9, which is consistent with a lower peak temperature for OC release using in IMPROVE (550°C vs. 850°C or 870°C). Accordingly, EC determined by IMPROVE was the highest, followed by ECT9 and NIOSH. Since the ECT9 method yielded the highest TC, its EC result was greater than NIOSH.

The difference of the protocols is mainly due to a portion of organic compounds evolve at relatively high temperatures (Subramanian *et al.*, 2006). It could also be slightly affected by the difference of detection methods, since only transmittance method could detect the charred POC inside quartz filter. Nonetheless, this reason still has low impact, as the emissions directly from engine exhaust have not been oxidized in the atmosphere and the POC formation was low ($<$ 5% of TC) for all three protocols used. Given the expected analytical uncertainties in any single OC/EC analysis, we use the average values of three protocols for each sample (Table S4) in the remainder of the results below. More confidence may also be gained by averaging the results given their differences imply some analytical uncertainty in the OC and EC measurements.

3.2 OC and EC Emission Factors (EF)

OC and EC EFs in μg C km^{-1} for each vehicle and test cycle are given in Table 1. The OC EFs for the three engine conditions during the FTP-75 and FTP-72 drive cycles were comparable and lower than the US06 drive cycle. The EFs between the GDI, GDI+GPF and PFI during the FTP-75 drive cycle were found to differ by less than 36%. Similar quantities and variations were found during the FTP-72 cycle. In contrast, under the US06 drive cycle the OC EFs were larger, especially from the PFI engine, and there was considerable variability among the vehicles. Specifically, the OC EFs for the GDI and PFI vehicles were 1455 ± 234 and 3581 ± 82 μg C km^{-1}, respectively, which were 3.7 and 15.8 times higher than that of FTP-72 test cycle. As both US06 and FTP-72 are hot-start cycles, this higher emission rate for OC is likely due to the aggressive driving pattern. This is consistent with previous measurements on the same vehicles which also showed significantly higher emissions from the PFI vehicle during very aggressive driving conditions compared to the

Table 1. Emission factor of OC and EC from vehicles under different test cycles (μg C km^{-1}). The averaged value measured by three different thermal optical protocols and standard deviation among them is provided.

Cycles	GDI		GDI + GPF		PFI	
	OC	EC	OC	EC	OC	EC
FTP-75	311 ± 44	4862 ± 185	335 ± 19	83 ± 18	213 ± 19	321 ± 24
FTP-72	256 ± 6	670 ± 14	441 ± 55	10 ± 18	285 ± 48	19 ± 33
US06	1455 ± 234	2933 ± 418	561 ± 82	10 ± 17	3581 ± 82	410 ± 196

GDI counterpart (Chan *et al.*, 2014, 2012, 2013). This is likely related to the different fuel injection methods of the two types of vehicles. During very demanding conditions (e.g., US06 cycle), the continued increase in fuel injection for the PFI vehicle significantly leads to incomplete vaporization of the fuel, thus worsening the emissions. In contrast, the switch from stratified-charge mode to the homogeneous-charge mode in the GDI engine during very demanding conditions allows the GDI vehicle to provide the needed power without significantly worsening the emissions (Chan *et al.*, 2014, 2013). The OC EF from the PFI engine was more-sensitive to the cycles, similar to what has been observed elsewhere (He *et al.*, 2018). Comparing GDI + GPF to GDI, OC decreased significantly with the addition of the GPF in the US06 cycle because some of the OC was likely in the particle phase and thereby captured by the GPF. For the FTP-72 drive cycles, there was a increase in OC emissions when using a GPF. A previous study has suggested that this could be a result of small and limited soot regeneration in the GPF (Chan *et al.*, 2016). Such an increase in emissions is likely to be compensated partly by the decrease in emissions during cold-start mode, and therefore is not that evident during the FTP-75 drive cycle (Chan *et al.*, 2013).

The EC EFs of the GDI vehicle during the FTP-75, FTP-72 and US06 cycles were 14.1, 65.9 and 6.2 times higher than that of PFI vehicle, respectively. The effect of the GPF on the GDI emissions was significant, decreasing EC by at least 98% in each test cycle, consistent with all previous measurements (Chan *et al.*, 2014, 2013). Similar results of up to a 99% decrease in soot emissions was observed for other GDI vehicles installed with a GPF (McCaffery *et al.*, 2020). Consistent with this, Jang *et al.* (2018) reported that particle numbers also decreased, but the extent varied by test cycle.

Unlike OC, for which there are relatively few publications comparing GDI and PFI engines, more has been reported for EC or BC. Zimmerman *et al.* (2016b) reviewed the literature and found that the mean BC emission level from GDI vehicles (around 1.5 mg $mile^{-1}$) was four times more than that of PFI vehicles (around 0.3 mg $mile^{-1}$). Chan *et al.* (2014) previously tested (FTP-75) the same two vehicles studied in this paper with a focus on *in situ* black carbon (BC) measurements and observed that the ratios of BC from GDI versus PFI vehicles were in the range of 7.8–18 at 22°C. Saliba *et al.* (2017) found that the EC ratio of the GDI versus PFI engine was 4.8 and 3.1 for ultra-low-emission vehicles and super ultra-low-emission vehicles, respectively.

Different injection and combustion conditions for GDI and PFI engines are known to lead to changes in OC and EC emissions. In GDI engines, liquid fuel accumulation on the piston and cylinder after injection (Maricq *et al.*, 2013) causes a less uniform mixture of air and fuel compared to PFI vehicles during cold start (e.g., FTP-75 cycle) (Chan *et al.*, 2014) causing more emissions for both EC and OC. Different injection and combustion situations also occur for aggressive driving cycles (e.g., US06). Specifically, for GDI vehicles extra load is needed during acceleration in the test cycles and therefore the engine operation mode changes from homogeneous-charge to stratified-charge, causing a heterogeneous air-fuel mixture (Zhao *et al.*, 1999; Barone *et al.*, 2012). For PFI vehicles, enrichment of the fuel mixture under high load leads to incomplete vaporization of fuel (Chan *et al.*, 2014, 2013).

3.3 Characteristics of Vehicle Semivolatile and Particle Phase OC

While the differences in EC emissions among engine configurations were as expected, the OC emission differences were more complex. A more-detailed comparison of the OC emissions detected on the QBT and on the Q filters after subtracting the OC on the QBT (Q-QBT) are presented in Figs. 2(a–c). OC on the QBT from the GDI engine, which likely represents gas phase SVOC emissions

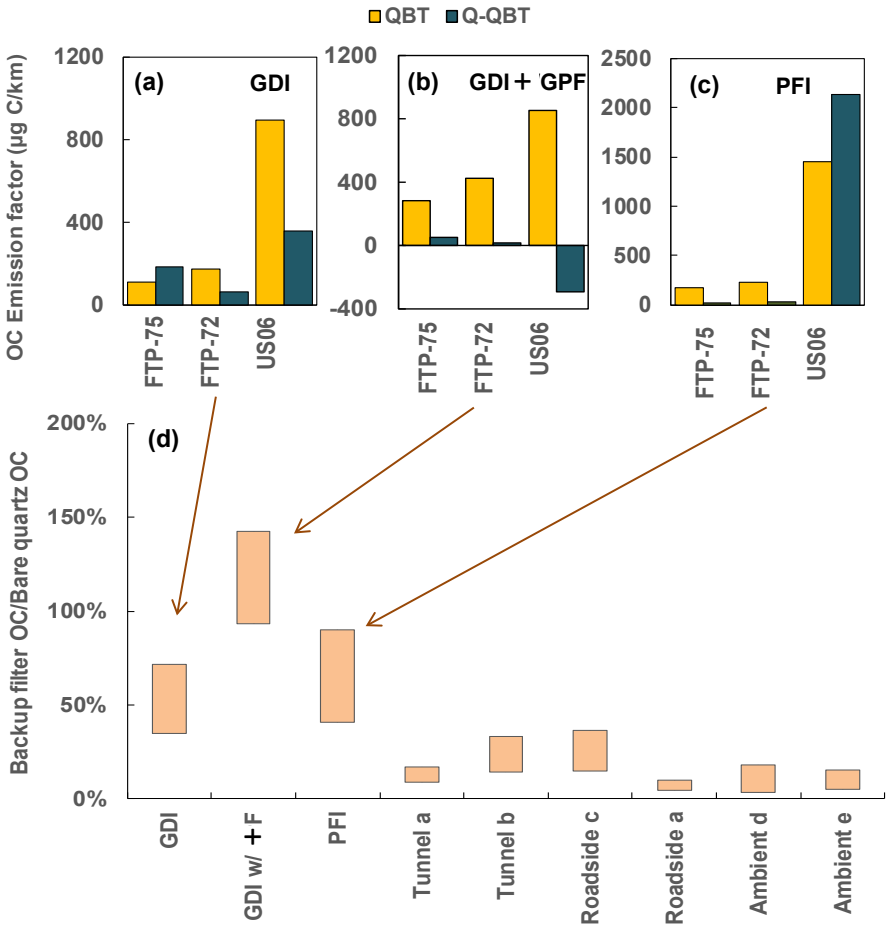

Fig. 2. OC emission factors from backup and bare quartz filters, and their ratio comparison with other types of samples. The figure (a), (b) and (c) shows OC emission factors obtained by Q and Q- QBT from three vehicle test settings (note the different y-axis scales). The (d) is comparison of OC QBT/Q in this study with references of different ambient sampling locations. The references reported measure OC using a TOR method with maximum inert mode temperature of 550°C (Cheng *et al.*, 2010; Chen *et al.*, 2010; Zhu *et al.*, 2012; Cheng *et al.*, 2009) and 580°C (Watson *et al.*, 2009).

and particle evaporation, was 70-80% lower than that of the PFI engine for all three driving cycles. In contrast, OC derived from Q-QBT, which likely corresponds to particle phase, was a factor of 5–6 higher for GDI vs. PFI during the FTP-75 and FTP-72 cycles, but much lower, by 85%, during US06 conditions.

There are two main sources of organic compounds from gasoline vehicle emissions. One is incomplete volatilized fuel droplets, which forms at the combustion temperature boundary layer, and has a greater proportion in the gas phase (Jiang *et al.*, 2018), implying it will predominantly be seen on QBT. The other is incomplete combustion of fuel, which occurs when an inhomogeneous mixture of fuel and air is pyrolyzed during combustion (Chan *et al.*, 2014), which is more likely to form particle phase compounds (e.g., PAHs) (Miersch *et al.*, 2019) and thus be detected on Q. The results in Fig. 2(d) suggest that the OC emissions from the PFI engine were more volatile than those from the GDI engine. This was clearly seen in the results of the most volatile OC fraction on QBT (OC1 by the IMPROVE method, which has the lowest heating temperature for OC1 among the protocols) (Table S5). The OC1 on QBT was 30.4 and 47.8 µg km^{-1} for PFI vehicles during the FTP-75 and FTP-72 cycles, which was 31 and 34 times higher than that of GDI vehicles, respectively (Table S5). The THC measurements (Table S2) show that the greater amounts of volatile/gas phase OC from PFI engines, captured in the quartz filter measurements (Fig. 2), extended into the VOC emissions. Specifically, THC emissions were 40% and 50% higher from the PFI engine during the

FTP-75 and FTP-72 cycles, respectively. A similar trend of higher THC concentrations from PFI engines was also observed in tests conducted for LEV1 and LEV2 strategies (Saliba *et al.*, 2017). This behavior for PFI indicates that the OC was more-likely to be due to volatilized fuel, thus distributing more in the gas phase (collected on QBT).

The higher Q-QBT associated with the cold-start FTP-75 cycle of the GDI engine could be due to formation of pyrolyzed particles caused by the 'wall-effect' of liquid fuel accumulating on the wall of the cylinder (Chan *et al.*, 2014; Maricq *et al.*, 2013). During the aggressive test cycle (US06) the OC1 measured by the IMPROVE method on QBT from the PFI engine was 65% higher than the GDI vehicle, which could be a result of excessive fuel being injected in the PFI engine than in the GDI engine (Jiang *et al.*, 2018). This explanation is also consistent with the larger EC EFs for GDI vs. PFI discussed above.

Comparing GDI and GDI+GPF, more OC on the QBT was observed when the GPF was added during FTP-75 and FTP-72 cycles (Fig. 2). Most of the increase on the QBT came from the more-volatile OC1 fraction; ~67 times higher after GPF installation (Table S5). A possible explanation is reactions on the surface of the GPF which converted some of the most volatile gas phase OC, including VOCs (i.e., THC), to less volatile organics that can then be adsorbed on the QBT. Given the relatively large amount of hydrocarbon emissions, conversion of a small fraction could have large impacts on the OC available to adsorb on the QBT. This GPF-induced production of SVOC and possibly particle phase OC is consistent with several other studies (Zhang *et al.*, 2016; Robinson *et al.*, 2007). Munoz *et al.* (2018) also reported higher PAH emissions in GDI exhaust following a GPF. Clearly, the influence of the GPF on vehicle OC emissions is complex and needs to be better understood, although it was highly effective for reducing EC and non-volatile OC. Continuous GPF regeneration adds further complexity, although the majority of the EC and OC collected is converted to CO_2 or CO given the availability of oxygen (Munoz *et al.*, 2018).

Fig. 2(d) also shows the proportion of OC on QBT versus Q in this study compared to similar measurements from heavily impacted locations, such as near-road and tunnel studies, to regional ambient air. The QBT/Q values in our emission measurements are significantly higher than studies in a tunnel, at roadside and ambient environments (Cheng *et al.*, 2010; Chen *et al.*, 2010; Zhu *et al.*, 2012; Cheng *et al.*, 2009), implying a greater proportion of the more volatile OC compounds in the fresh exhaust. Under the field study conditions shown, the reduction in the proportion of gas phase OC relative to the more non-volatile particle OC could be due to cooling and condensation on particles and other surfaces and/or rapid reaction forming less volatile particle OC (i.e., SOA) (Zhang *et al.*, 2016). Zimmerman *et al.* (2016a) observed a rapid growth of nano particles from a GDI vehicle as its exhaust plume transported away from the road suggesting condensation of low volatility gas phase organic compounds.

Large amounts of gas phase OC emitted by vehicles have been reported by others. Zhao *et al.* (2016) measured the total intermediate volatility organic compounds (IVOC) and SVOC from gasoline vehicles and found that IVOC and SVOC collected on absorbent tubes contributed 47% and 53% of the total organics collected on the quartz filter, respectively. Li *et al.* (2016) found that in traffic tunnel and dynamometer tests the OC collected on a bare quartz filter consisted of only 12% low volatility OC, while 60–80% was SVOC. Lu *et al.* (2018) suggested that the distribution of particle phase OC, SVOC and IVOC is ultimately determined by the combination of the volatility distribution in the emissions and the ambient temperature environment. Our measurements clearly show that, for the conditions created in the CVS (T = 22°C), a large fraction of the overall OC consists of the more volatile compounds remaining in the gas phase.

In addition to complicating the measurement of actual particle OC emissions, the gas phase OC is potentially important to subsequent particle OC formation after emission through atmospheric transformations. Lu *et al.* (2018) measured IVOC in gasoline and diesel vehicle exhaust with an *in situ* gas chromatograph after the emitted particles were removed by a front filter, finding that the IVOC contributed about one third of total SOA yields in non-methane organic gases emissions. This suggested that IVOC was an important source of SOA formation in the atmosphere. Indeed, IVOC has been found to readily form SOA in smog chamber studies (Jathar *et al.*, 2014). Ultimately this implies that after emission from the tailpipe the volatility of the gas phase OC decreases and particle OC increases, including SOA formed through oxidation of IVOC (Jathar *et al.*, 2014; Zhang *et al.*, 2016), consistent with the ratios shown in the Fig. 2(d).

4 CONCLUSIONS AND IMPLICATIONS

Carbonaceous particle samples from three vehicle settings (GDI, GDI + GPF, and PFI) were collected under different cycles (FTP-75, FTP-72 and US06) and measured with three protocols (IMPROVE, NIOSH and ECT9). Comparing the protocols, the IMPROVE and NIOSH gave similar TC, while the ECT9 resulted in higher TC. The IMPROVE protocol determined OC to be the lowest and EC to be the highest among the protocols, probably due to incomplete OC evaporation at relatively low inert mode peak temperature.

The OC EFs for the three engine conditions during the FTP-75 and FTP-72 drive cycles were comparable and lower than that of US06 drive cycle. The OC EF for PFI vehicle during US06 cycle increased to 3581 μg C km^{-1}, which was 11 times higher than that of FTP-72 cycle with the same vehicle and 1.5 times higher than GDI vehicle at the same cycle. The EC EFs of the GDI vehicle were 6.2 to 14.1 times higher than PFI vehicle, and the EC emissions could be reduced by at least 98% in each test cycle by applying GPF.

OC on the QBT from GDI vehicle emissions was 70-80% lower than that of the PFI vehicle, and this value for the most volatile fraction OC1 could even reach 97% during FTP-72 cycle, indicating higher volatility of PFI vehicle emissions. Generally, the QBT/Q value in our vehicle emissions measurements were much higher than other roadside or ambient air studies, suggesting more volatile OC compounds in the fresh vehicle exhaust. More OC on the QBT was observed after the GPF applied on the GDI vehicle during FTP-75 and FTP-72 cycles, and the OC1 also increased around 67 times, implying reactions on the surface of GPF could probably produce new SVOC.

The particle and gas phase organic compounds from both GDI and PFI engines under various driving cycles requires further study in order to quantify their impact on environmental pollution. GDI vehicles are believed to have more PM emissions than PFI vehicles, however, this behavior cannot be generalized. Our results indicate that the PFI vehicle can cause larger OC emissions under aggressive cycles with excessive fuel injection. The effect of GPFs on particle removal also needs to be more-comprehensively evaluated, since it increased the SVOC emissions though particle emissions were decreased. Our study suggests oxidation and condensation of gas phase organic compounds occurs as the exhaust passes through the GPF. This enhanced effect of GPF on SVOC could also induce more SOA formation. With wider GPF application in coming years, further studies on GPF performance and their effects on SOA are needed.

ACKNOWLEDGEMENTS

The authors would like to acknowledge the contribution of the Emission Research and Measurement Section (ERMS) staff for their assistance in conducting this vehicle emissions research project. This work was sponsored by the Science and Technology Planning Project of Jiangsu Provincial Environmental Protection Group (JSEP-TZ-2021-2003-RE and JSEP-TZ-2021-2002-RE) and Program of Energy Research and Development from Natural Resources Canada (PERD ECOII program).

SUPPLEMENTARY MATERIAL

Supplementary material for this article can be found in the online version at https://doi.org/10.4209/aaqr.220032

REFERENCES

Andreae, M.O., Jones, C.D., Cox, P.M. (2005). Strong present-day aerosol cooling implies a hot future. Nature 435, 1187–1190. https://doi.org/10.1038/nature03671

Barone, T.L., Storey, J.M.E., Youngquist, A.D., Szybist, J.P. (2012). An analysis of direct-injection spark-ignition (DISI) soot morphology. Atmos. Environ. 49, 268–274. https://doi.org/10.1016/j.atmosenv.2011.11.047

Birch, M.E., Cary, R.A. (1996). Elemental carbon-based method for monitoring occupational

exposures to particulate diesel exhaust. Aerosol Sci. Technol. 25, 221–241. https://doi.org/10.1080/02786829608965393

Cai, T., Zhang, Y., Fang, D., Shang, J., Zhang, Y., Zhang, Y. (2017). Chinese vehicle emissions characteristic testing with small sample size: Results and comparison. Atmos. Pollut. Res. 8, 154–163. https://doi.org/10.1016/j.apr.2016.08.007

Chan, T.W., Meloche, E., Kubsh, J., Rosenblatt, D., Brezny, R., Rideout, G. (2012). Evaluation of a gasoline particulate filter to reduce particle emissions from a gasoline direct injection vehicle. SAE Int. J. Fuels Lubr. 5, 1277–1290. https://doi.org/10.4271/2012-01-1727

Chan, T.W., Meloche, E., Kubsh, J., Brezny, R., Rosenblatt, D., Rideout, G. (2013). Impact of ambient temperature on gaseous and particle emissions from a direct injection gasoline vehicle and its implication on particle filtration. SAE Int. J. Fuels Lubr. 6, 350–371. https://doi.org/10.4271/2013-01-0527

Chan, T.W., Meloche, E., Kubsh, J., Brezny, R. (2014). Black carbon emissions in gasoline exhaust and a reduction alternative with a gasoline particulate filter. Environ. Sci. Technol. 48, 6027–6034. https://doi.org/10.1021/es501791b

Chan, T.W., Saffaripour, M., Liu, F., Hendren, J., Thomson, K.A., Kubsh, J., Brezny, R., Rideout, G. (2016). Characterization of real-time particle emissions from a gasoline direct injection vehicle equipped with a catalyzed gasoline particulate filter during filter regeneration. Emiss. Control Sci. Technol. 2, 75–88. https://doi.org/10.1007/s40825-016-0033-3

Chao, M., Wu, L., Mao, H.J., Fang, X., Wei, N., Zhang, J., Yang, Z., Zhang, Y., Lv, Z., Yang, L. (2020). Transient characterization of automotive exhaust emission from different vehicle types based on on-road measurements. Atmosphere 11, 64–102. https://doi.org/10.3390/atmos11010064

Chen, S.C., Tsai, C.J., Huang, C.Y., Chen, H.D., Chen, S.J., Lin, C.C., Tsai, J.H., Chou, C.C.K., Lung, S.C.C., Huang, W.R., Roam, G.D., Wu, W.Y., Smolik, J., Dzumbova, L. (2010). Chemical mass closure and chemical characteristics of ambient ultrafine particles and other PM fractions. Aerosol Sci. Technol. 44, 713–723. https://doi.org/10.1080/02786826.2010.486385

Cheng, Y., He, K.B., Duan, F.K., Ma, Y.L., Tan, J.H. (2009). Positive sampling artifact of carbonaceous aerosols and its influence on the thermal-optical split of OC/EC. Atmos. Chem. Phys. 9, 7243–7256. https://doi.org/10.5194/acp-9-7243-2009

Cheng, Y., Lee, S.C., Ho, K.F., Fung, K. (2010). Positive sampling artifacts in particulate organic carbon measurements in roadside environment. Environ. Monit. Assess. 168, 645–656. https://doi.org/10.1007/s10661-009-1140-1

Cheng, Y., He, K.B., Duan, F.K., Du, Z.Y., Zheng, M., Ma, Y.L. (2014). Ambient organic carbon to elemental carbon ratios: Influence of the thermal-optical temperature protocol and implications. Sci. Total Environ. 468–469, 1103–1111. https://doi.org/10.1016/j.scitotenv.2013.08.084

Chiappini, L., Verlhac, S., Aujay, R., Maenhaut, W., Putaud, J.P., Sciare, J., Jaffrezo, J.L., Liousse, C., Galy-Lacaux, C., Alleman, L.Y., Panteliadis, P., Leoz, E., Favez, O. (2014). Clues for a standardised thermal-optical protocol for the assessment of organic and elemental carbon within ambient air particulate matter. Atmos. Meas. Tech. 7, 1649–1661. https://doi.org/10.5194/amt-7-1649-2014

Chow, J.C., Watson, J.G., Crow, D., Lowenthal, D.H., Merrifield, T. (2001). Comparison of IMPROVE and NIOSH carbon measurements. Aerosol Sci. Technol. 34, 23–34. https://doi.org/10.1080/02786820119073

Chow, J.C., Watson, J.G., Louie, P.K., Chen, L.W., Sin, D. (2005). Comparison of $PM_{2.5}$ carbon measurement methods in Hong Kong, China. Environ. Pollut. 137, 334–344. https://doi.org/10.1016/j.envpol.2005.01.006

Giannoni, M., Calzolai, G., Chiari, M., Cincinelli, A., Lucarelli, F., Martellini, T., Nava, S. (2016). A comparison between thermal-optical transmittance elemental carbon measured by different protocols in $PM_{2.5}$ samples. Sci. Total Environ. 571, 195–205. https://doi.org/10.1016/j.scitotenv.2016.07.128

Gordon, T.D., Presto, A.A., Nguyen, N.T., Robertson, W.H., Na, K., Sahay, K.N., Zhang, M., Maddox, C., Rieger, P., Chattopadhyay, S., Maldonado, H., Maricq, M.M., Robinson, A.L. (2014). Secondary organic aerosol production from diesel vehicle exhaust: Impact of aftertreatment, fuel chemistry and driving cycle. Atmos. Chem. Phys. 14, 4643–4659. https://doi.org/10.5194/acp-14-4643-2014

He, L., Hu, J., Zhang, S., Wu, Y., Zhu, R., Zu, L., Bao, X., Lai, Y., Su, S. (2018). The impact from the direct injection and multi-port fuel injection technologies for gasoline vehicles on solid particle

number and black carbon emissions. Appl. Energy 226, 819−826. https://doi.org/10.1016/j.apenergy.2018.06.050

Huang, L., Brook, J.R., Zhang, W., Li, S.M., Graham, L., Ernst, D., Chivulescu, A., Lu, G. (2006). Stable isotope measurements of carbon fractions (OC/EC) in airborne particulate: A new dimension for source characterization and apportionment. Atmos. Environ. 40, 2690−2705. https://doi.org/10.1016/j.atmosenv.2005.11.062

Jang, J., Lee, J., Choi, Y., Park, S. (2018). Reduction of particle emissions from gasoline vehicles with direct fuel injection systems using a gasoline particulate filter. Sci. Total Environ. 644, 1418−1428. https://doi.org/10.1016/j.scitotenv.2018.06.362

Jathar, S.H., Gordon, T.D., Hennigan, C.J., Pye, H.O.T., Pouliot, G., Adams, P.J., Donahue, N.M., Robinson, A.L. (2014). Unspeciated organic emissions from combustion sources and their influence on the secondary organic aerosol budget in the united states. Proc. Natl. Acad. Sci. U.S.A. 111, 10473−10478. https://doi.org/10.1073/pnas.1323740111

Jiang, C., Li, Z., Qian, Y., Wang, X., Zhang, Y., Lu, X. (2018). Influences of fuel injection strategies on combustion performance and regular/irregular emissions in a turbocharged gasoline direct injection engine: Commercial gasoline versus multi-components gasoline surrogates. Energy 157, 173−187. https://doi.org/10.1016/j.energy.2018.05.160

Jung, J., Kim, Y.J., Lee, K.Y., Kawamura, K., Hu, M., Kondo, Y. (2011). The effects of accumulated refractory particles and the peak inert mode temperature on semi-continuous organic carbon and elemental carbon measurements during the CAREBeijing 2006 campaign. Atmos. Environ. 45, 7192−7200. https://doi.org/10.1016/j.atmosenv.2011.09.003

Khan, B., Hays, M.D., Geron, C., Jetter, J. (2012). Differences in the OC/EC ratios that characterize ambient and source aerosols due to thermal-optical analysis. Aerosol Sci. Technol. 46, 127−137. https://doi.org/10.1080/02786826.2011.609194

Li, X., Dallmann, T.R., May, A.A., Tkacik, D.S., Lambe, A.T., Jayne, J.T., Croteau, P.L., Presto, A.A. (2016). Gas-particle partitioning of vehicle emitted primary organic aerosol measured in a traffic tunnel. Environ. Sci. Technol. 50, 12146−12155. https://doi.org/10.1021/acs.est.6b01666

Lim, J., Lim, C., Jung, S. (2021). Characterizations of size-segregated ultrafine particles in diesel exhaust. Aerosol Air Qual. Res. 21, 200356. https://doi.org/10.4209/aaqr.200356

Lin, Y.C., Li, Y.C., Amesho, K.T.T., Chou, F.C., Cheng, P.C. (2020). Filterable $PM_{2.5}$, metallic elements, and organic carbon emissions from the exhaust of diesel vehicles. Aerosol Air Qual. Res. 20, 1319−1328. https://doi.org/10.4209/aaqr.2020.02.0081

Lu, Q., Zhao, Y., Robinson, A.L. (2018). Comprehensive organic emission profiles for gasoline, diesel, and gas-turbine engines including intermediate and semi-volatile. Atmos. Chem. Phys. 18, 17637–17654. https://doi.org/10.5194/acp-2018-752

Maricq, M.M., Szente, J.J., Jahr, K. (2012). The impact of ethanol fuel blends on PM emissions from a light-duty GDI vehicle. Aerosol Sci. and Tech. 46, 576−583. https://doi.org/10.1080/02786826.2011.648780

Maricq, M.M., Szente, J.J., Adams, J., Tennison, P., Rumpsa, T. (2013). Influence of mileage accumulation on the particle mass and number emissions of two gasoline direct injection vehicles. Environ. Sci. Technol. 47, 11890−11896. https://doi.org/10.1021/es402686z

May, A.A., Presto, A.A., Hennigan, C.J., Nguyen, N.T., Gordon, T.D., Robinson, A.L. (2013). Gas-particle partitioning of primary organic aerosol emissions: (1) gasoline vehicle exhaust. Atmos. Environ. 77, 128−139. https://doi.org/10.1016/j.atmosenv.2013.04.060

McCaffery, C., Zhu, H., Li, C., Durbin, T.D., Johnson, K.C., Jung, H., Brezny, R., Geller, M., Karavalakis, G. (2020). On-road gaseous and particulate emissions from GDI vehicles with and without gasoline particulate filters (GPFs) using portable emissions measurement systems (PEMS). Sci. Total Environ. 710, 136366. https://doi.org/10.1016/j.scitotenv.2019.136366

Miersch, T., Czech, H., Stengel, B., Abbaszade, G., Orasche, J., Sklorz, M., Streibel, T., Zimmermann, R. (2019). Composition of carbonaceous fine particulate emissions of a flexible fuel DISI engine under high velocity and municipal conditions. Fuel 236, 1465−1473. https://doi.org/10.1016/j.fuel.2018.09.136

Munoz, M., Haag, R., Zeyer, K., Mohn, J., Comte, P., Czerwinski, J., Heeb, N.V. (2018). Effects of four prototype gasoline particle filters (GPFs) on nanoparticle and genotoxic PAH emissions of a gasoline direct injection (GDI) vehicle. Environ. Sci. Technol. 52, 10709−10718. https://doi.org/10.1021/acs.est.8b03125

Preble, C.V., Dallmann, T.R., Kreisberg, N.M., Hering, S.V., Harley, R.A., Kirchstetter, T.W. (2015). Effects of particle filters and selective catalytic reduction on heavy-duty diesel drayage truck emissions at the port of Oakland. Environ. Sci. Technol. 49, 8864−8871. https://doi.org/10.1021/acs.est.5b01117

Robinson, A.L., Donahue, N.M., Shrivastava, M.K., Weitkamp, E.A., Sage, A.M., Grieshop, A.P., Lane, T.E., Pierce, J.R., Pandis, S.N. (2007). Rethinking organic aerosols: Semivolatile emissions and photochemical aging. Science 315, 1259−1262. https://doi.org/10.1126/science.1133061

Saliba, G., Saleh, R., Zhao, Y., Presto, A.A., Lambe, A.T., Frodin, B., Sardar, S., Maldonado, H., Maddox, C., May, A.A., Drozd, G.T., Goldstein, A.H., Russell, L.M., Hagen, F., Robinson, A.L. (2017). Comparison of gasoline direct-injection (GDI) and port fuel injection (PFI) vehicle emissions: Emission certification standards, cold-start, secondary organic aerosol formation potential, and potential climate impacts. Environ. Sci. Technol. 51, 6542−6552. https://doi.org/10.1021/acs.est.6b06509

Subramanian, R., Khlystov, A.Y., Robinson, A.L. (2006). Effect of peak inert-mode temperature on elemental carbon measured using thermal-optical analysis. Aerosol Sci. Technol. 40, 763−780. https://doi.org/10.1080/02786820600714403

Valverde, V., Giechaskiel, B. (2020). Assessment of gaseous and particulate emissions of a Euro 6d-Temp diesel vehicle driven >1300 km including six diesel particulate filter regenerations. Atmosphere 11, 645−669. https://doi.org/10.3390/atmos11060645

Watson, J.G., Chow, J.C., Chen, L.W. A., Frank, N.H. (2009). Methods to assess carbonaceous aerosol sampling artifacts for improve and other long-term networks. J. Air Waste Manage. Assoc. 59, 898−911. https://doi.org/10.3155/1047-3289.59.8.898

Zhang, J., He, K., Ge, Y., Shi, X. (2009). Influence of fuel sulfur on the characterization of PM_{10} from a diesel engine. Fuel 88, 504–510. https://doi.org/10.1016/j.fuel.2008.09.001

Zhang, J., Fan, X., Graham, L., Chan, T.W., Brook, J.R. (2013). Evaluation of an annular denuder system for carbonaceous aerosol sampling of diesel engine emissions. J. Air Waste Manage. Assoc. 63, 87−99. https://doi.org/10.1080/10962247.2012.739582

Zhang, J., Dabek-Zlotorzynska, E., Liggio, J., Stroud, C.A., Charland, J.P., Brook, J.R. (2016). Use of the integrated organic gas and particle sampler to improve the characterization of carbonaceous aerosol in the near-road environment. Atmos. Environ. 126, 192−199. https://doi.org/10.1016/j.atmosenv.2015.11.051

Zhao, F., Lai, M.C., Harrington, D.L. (1999). Automotive spark-ignited direct-injection gasoline engines. Prog. Energy Combust. Sci. 25, 437−562. https://doi.org/10.1016/S0360-1285(99)00004-0

Zhao, Y., Nguyen, N.T., Presto, A.A., Hennigan, C.J., May, A.A., Robinson, A.L. (2016). Intermediate volatility organic compound emissions from on-road gasoline vehicles and small off-road gasoline engines. Environ. Sci. Technol. 50, 4554−4563. https://doi.org/10.1021/acs.est.5b06247

Zhu, C.S., Tsai, C.J., Chen, S.C., Cao, J.J., Roam, G.D. (2012). Positive sampling artifacts of organic carbon fractions for fine particles and nanoparticles in a tunnel environment. Atmos. Environ. 54, 225−230. https://doi.org/10.1016/j.atmosenv.2012.02.060

Zimmerman, N., Wang, J.M., Jeong, C.H., Ramos, M., Hilker, N., Healy, R.M., Sabaliauskas, K., Wallace, J.S., Evans, G.J. (2016a). Field measurements of gasoline direct injection emission factors: Spatial and seasonal variability. Environ. Sci. Technol. 50, 2035−2043. https://doi.org/10.1021/acs.est.5b04444

Zimmerman, N., Wang, J.M., Jeong, C.H., Wallace, J.S., Evans, G.J. (2016b). Assessing the climate trade-offs of gasoline direct injection engines. Environ. Sci. Technol. 50, 8385−8392. https://doi.org/10.1021/acs.est.6b01800